7-1-2008

A Computational Approach to Optimal Damping Controller Design for a GCSC

Swakshar Ray

Ganesh K. Venayagamoorthy
Missouri University of Science and Technology

Edson H. Watanabe

A Computational Approach to Optimal Damping Controller Design for a GCSC

Swakshar Ray, *Student Member, IEEE*, Ganesh Kumar Venayagamoorthy, *Senior Member, IEEE*, and
Edson H. Watanabe, *Senior Member, IEEE*

Abstract—This paper presents a computational approach for an offline measurement-based design of an optimal damping controller using adaptive critics for a new type of flexible ac transmission system device—the gate-controlled series capacitor (GCSC). Remote measurements are provided to the controller to damp out system modes. The optimal controller is developed based on the heuristic dynamic programming (HDP) approach. Three multilayer-perceptron neural networks are used in the design—the identifier/model network to identify the dynamics of the power system, the critic network to evaluate the performance of the damping controller, and the controller network to provide optimal damping. This measurement-based technique provides an alternative to the classical linear model-based optimal control design. The eigenvalue analysis of the closed-loop system is performed with time-domain responses using the Prony method. An analysis of the simulation results shows potential of the HDP-based optimal damping controller on a GCSC for enhancing the stability of the power system.

Index Terms—Flexible ac transmission systems (FACTS), gate-controlled series capacitor (GCSC), heuristic dynamic programming, neurocontroller, Prony method, remote measurement, wide-area control.

I. INTRODUCTION

TODAY'S deregulated market demands more generation, with less investment in transmission capacity and more power transfer through existing transmission corridors. The flexible ac transmission systems (FACTS) devices can provide transmission control through dynamical control of real and reactive power flow. Not only can it satisfy the market requirements but also may improve the transient performance of the power system. Most commonly used FACTS devices are shunt-connected devices. But the series-connected devices can provide control of line flow and subsequent damping of power-flow oscillations. These series FACTS devices include thyristor-controlled series capacitor (TCSC) and static synchronous series compensator (SSSC), etc. There are a few installations of TCSC in the world [1], [2]. The Brazilian North

South Interconnection with a TCSC to damp out low-frequency interarea oscillation is one good example of TCSC installation since it leads to very important expansion in the Brazilian power system. Recently, a new series FACTS device, the gate-controlled series capacitor (GCSC), has been proposed [3]–[5] which has advantages over TCSC in regard to the size of the capacitor being smaller and that no reactor is required. Hence, it can be a less expensive solution in the future. The SSSC [6], [7] is a more complete device in terms of flexibility than the GCSC; however, its cost and complexity are much higher than GCSC.

Remote measurement-based control has shown significant improvement in damping interarea modes with TCSC, static var compensators (SVCs), and power system stabilizers (PSSs) [8]–[11]. Ideally, in a wide-area monitoring system (WAMS), global positioning system (GPS) synchronized time-stamped data are used. In today's technology, even in the worst scenarios, dedicated communication channels should not have more than 50-ms delay for the transmission of measured signals [12], [13]. But a robust controller design is not affected by a small delay. Therefore, signal transmission delay is no more of an important issue for designing remote-measurement-based wide-area controllers (WACs). In the near future, remote measurement-based WACs are expected to provide better stability and security to the interconnected power system. For the new GCSC FACTS device, a similar approach of remote measurement-based stabilizing control may provide a less expensive solution to low-frequency oscillations in the system. This paper investigates such a remote measurement-based technique for a GCSC.

With power systems that are highly nonlinear and time varying, the performances of the linear controllers degrade as the operating point and conditions of the system change, which justifies the need to retune the linear controllers. Though the retuning can provide a solution for permanent changes in the system, it is not feasible for temporary changes. To overcome this problem, researchers have proposed a different adaptive and robust control technique for nonlinear dynamic systems [14], [15] through classical methods. Computational methods, such as direct and indirect adaptive control, have also been discussed in [16] and [17]. Control designs using computational intelligence or intelligent controls of generator excitation, turbine systems, and earlier series and shunt FACTS devices have presented promising results [18], [19]. While adaptive control has its own advantages, it is difficult to prove their stability unconditionally. Hence, a robust optimal controller design is advantageous in this aspect because of its fixed parameters.
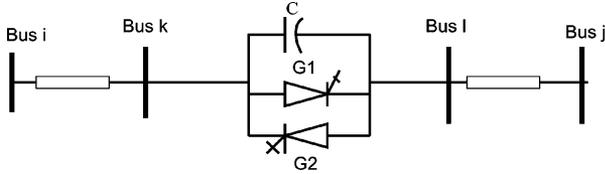
Fig. 1. Schematic diagram of a GCSC inserted between buses i and j in a transmission line.

Approximate dynamic-programming (ADP)-based adaptive critic design (ACD) is an alternative approach to classical designs in providing optimal control without the need for a detailed linear model (classical design) or online training (adaptive control) [20]–[23]. The heuristic dynamic programming (HDP) is the simplest in the family of ACD techniques applied to design an optimal controller [20]–[23]. This paper presents a remote measurement-based HDP-based optimal damping controller design for a GCSC to enhance damping of the power system oscillation during small and large disturbances.

The rest of this paper is organized as follows. Section II describes the structure and control of a simple GCSC. Section III presents the multimachine power system under study. Section IV describes the idea of remote measurement-based control. Section V presents the HDP optimal damping controller design. Section VI presents the results on the performance of the proposed controller using time-domain simulation and the evaluation of the damping performance using the Prony method. Finally, the conclusions and future work are given in Section VII.

II. GATE-CONTROLLED SERIES CAPACITOR

A. Architecture and Operation

The GCSC is composed of two antiparallel gate-controlled switches and a capacitor bank in series with the transmission line as shown by the single-line diagram in Fig. 1. If the switches are turned on all of the time, then the capacitor is bypassed and it does not provide any compensation. However, if the switches are turned off once per cycle at a determined blocking angle of a, the capacitor in series with the transmission line turns on and off alternately and a voltage V_c appears across the capacitor. The GCSC has a great advantage over TCSC as the blocking angle (α) can be varied continuously, thus varying the fundamental components of V_c. In contrast, the TCSC firing angle is discontinuous due to the zone in which a parallel resonance occurs between the thyristor-controlled reactor (TCR) and the capacitor [4].

In the GCSC, a blocking angle of $90°$ means that the capacitor is fully inserted and a blocking angle of $180°$ means that the capacitor is fully bypassed, making effective capacitive reactance zero. The dynamic control range for the reactance of a GCSC can be varied from 0 to $X_{\max}$ unlike TCSC where it can only vary between $X_{\min}$ to $X_{\max}$, where $X_{\min} > 0$. Also, GCSC does not need an extra reactor unlike the TCSC; this reduces the cost of the device. For these reasons, the GCSC might be a better solution in most situations than other controlled series compensators for future deployments. A different multimodular structure of the GCSC has been discussed in [5]. For simplicity, only the single module structure of GCSC is considered in this paper.
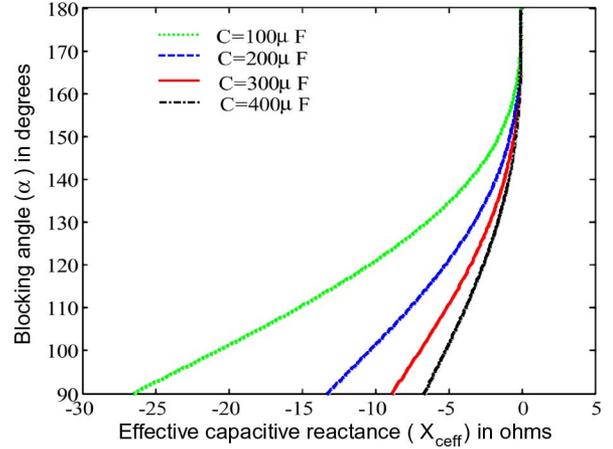

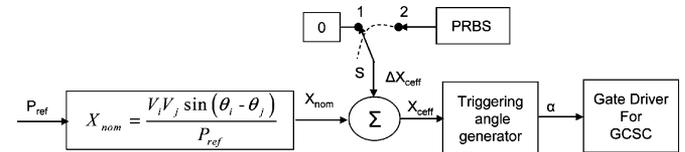Fig. 2. Plot for blocking angle versus effective capacitive compensation.

Fig. 3. Internal control block diagram for the GCSC (switch S is used to apply the PRBS signal as explained in Section VI-A).

The GCSC could be used in applications where fixed capacitive compensation—TCSC or SSSC—is used today, mainly to control power flow and provide damping to system oscillations. The GCSC can operate in an open-loop mode controlling the capacitive reactance added in series with the transmission line. It can also operate in a closed-loop mode where it controls the real power flow in the transmission line or maintains a constant compensation voltage. One interesting point is that GCSC can be used to retrofit existing fixed series capacitors just by adding controlled switches and its controllers.

B. Control

The control of a GCSC is difficult due to the wide saturation region in the relation of capacitive compensation reactance (X_{ceff}) and the blocking angle (α) as given in (1) and shown in Fig. 2

$$X_{\mathrm{ceff}} = \frac{X_c}{\pi}[2\alpha - 2\pi - \sin 2\alpha]. \qquad (1)$$

Here, X_c is the total installed reactance of the capacitor bank. Similar to most series capacitor-based FACTS devices, the internal control of the GCSC, shown in Fig. 3, provides a reactive compensation command (X_{ceff}) to the blocking angle generator. The blocking angle (α) is fed to the gate drivers of the GCSC. In the GCSC control, the control signal is applied to the gate driver only once in a cycle. To calculate the accurate firing angle by the controller, the time lag involved is less than $100\ \mu\mathrm{s}$ and the firing pulse generation takes 1–$2\ \mu\mathrm{s}$. Hence, the effective reactance of the GCSC capacitor can change within $100\ \mu\mathrm{s}$ after the controller provides the new reference signal. This small time lag can only cause a phase delay of 0.04–$0.08°$, which is small enough to be ignored for proper operation of the controller.

Unlike, the power-electronic switches in a TCSC, a GCSC triggering circuit provides blocking signals to the gates of
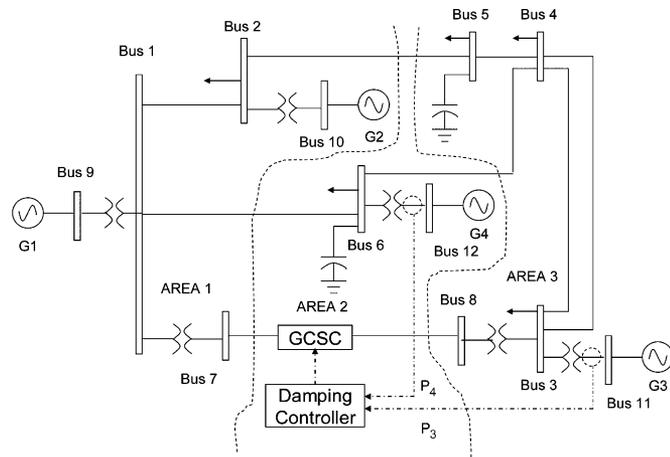
Fig. 4. Twelve-bus FACTS benchmark power system.

TABLE I
GCSC PARAMETERS AND RATING

PARAMETER	RATING
CAPACITOR REACTANCE/PHASE	$103 \, \Omega$
CAPACITANCE/PHASE	$28 \, \mu F$
MAX. REACTANCE	$103 \, \Omega$
DYNAMIC CONTROL RANGE	$0 - 103 \, \Omega$
MAX. FUNDAMENTAL VOLTAGE	59.7 KV
MAX. RMS VOLTAGE	59.7 KV
MAX. CAPACITOR CURRENT	4700 A
MAX. VALVE CURRENT	4700 A

the controlled switches instead of firing signals. The reactive compensation command (X_{ceff}) is generated from the requirement of active power flow in the transmission line (P_{ref}) during normal operation of fixed compensation. During disturbances, a stabilizing auxiliary control signal (ΔX) can be added to X_{ceff} to provide damping to the oscillating modes in a power system. The objective of this paper is to design a HDP-based optimal damping controller for a GCSC as elaborated in Sections IV and V.

III. MULTIMACHINE POWER SYSTEM

The 12 bus multimachine FACTS benchmark power system [24] used in this study is shown in Fig. 4. Bus 9 is the infinite or slack bus (G1). There are three geographic areas in the system with six 230-kV buses, two 345-kV buses, and four 22-kV generator buses. Area 1 consists of an infinite bus and generator 2 (G2), and area 2 consists of generator 4 (G4) and the area 3 has generator 3 (G3) and most of the loads. Each generator is equipped with an automatic voltage regulator (AVR), exciter for the field voltage control and governor and turbine for the frequency control. The GCSC is integrated in this system between buses 7 and 8 to provide control over real power flow. The location has been chosen from earlier studies published on the 12-bus system [24], [25], which shows that the best location for a series FACTS device is between buses 7 and 8 since it requires transferring a large amount of power. Even though all of the generators in the system are in one area, according to [25], the remote signals for FACTS supplementary control do help in damping even though there are PSSs in the system. This paper shows the effect of remote signal-based supplementary control to a GCSC for damping. The sizing of GCSC is chosen to provide up to 50% compensation of the line impedance (Table I). The power system with the GCSC is modeled in a PSCAD/EMTDC [26] environment with a time step of 50 μs. Hence, the switching effects of the GCSC can be included in the simulation.

IV. REMOTE MEASUREMENT-BASED WIDE-AREA CONTROL

In the last few decades, researchers have shown that the remote measurements or global signals can be used as inputs to the controller for providing better stabilizing control for power system applications. In a large multiarea power system

with several modes of oscillations, the remote measurements provide proper identification of modes which can be subsequently damped using wide-area control methods [8]–[11]. In the 12-bus FACTS benchmark system, there are three areas and three distinct modes associated with each generator. The least damped modes corresponding to 0.83 and 1.15 Hz are associated with generators G3 and G4, respectively. Hence, in this paper, the power flow through lines 3–11 (P_3) and 6–12 (P_4) have been selected as the remote measurements inputs to the damping controller. The damping controller is developed using these remote measurements to provide a stabilizing control signal to the GCSC in lines 7–8.

In the past, the remote measurement-based controller designs were not attractive due to the problem of delays in signal transmission. But with modern communication technology and dedicated channels for signal transmission, delay is less than 50 ms and is no longer regarded as a bottleneck in the design of wide-area controllers. In this work, the delay in measurement is assumed to be no more than 50 ms and is neglected in the design. But due to the inherent characteristics of the optimal controller, it is able to withstand small delays as shown in the results (Section VI-B).

V. HDP OPTIMAL NEUROCONTROLLER DESIGN

The optimal control design implemented in this paper is based on the HDP approach, a member of the ACD family [20]–[23]. ACDs are neural-network-based designs for optimization over time using combined concepts of reinforcement learning and approximate dynamic programming. ACDs use two neural networks—the critic and action networks to solve the Hamilton–Jacobi–Bellman equation of optimal control. The critic network approximates the cost-to-go function J of Bellman's equation of dynamic programming (2)

$$J(t) = \sum_{k=1}^{\infty} \gamma^k U(t+k) \tag{2}$$

where γ is a discount factor between 0 and 1, and $U(t)$ is a utility function or a local performance index. The action neural network also referred to as the actor in the ACD literature. This network provides optimal control to minimize or maximize the cost-to-go function J. It is referred to as the neurocontroller in this paper providing the optimal damping control signal to the GCSC. Several other ACD approaches such as the dual-
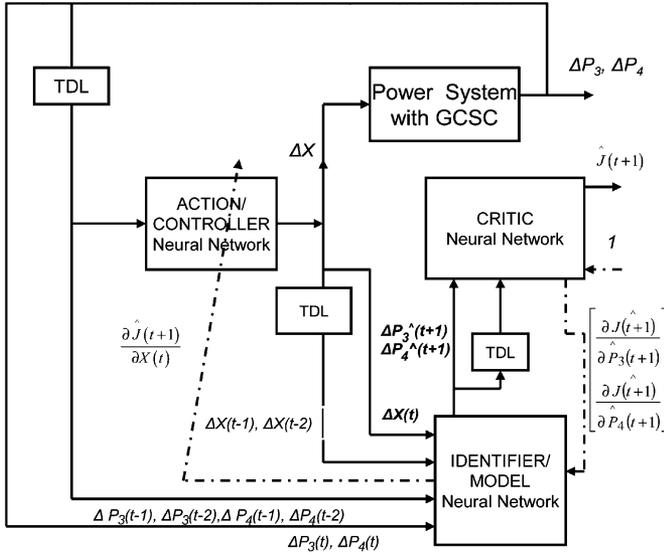
Fig. 5. HDP design of optimal neurocontroller (TDL is the time delay lines).

Fig. 6. MLP neural-network structure.

heuristic programming (DHP) and the global dual-heuristic programming (GDHP) exist [20]. The HDP design illustrated in Fig. 5 is used for the design of an optimal damping controller in this paper and is explained including the development of a model using a neural network (the neuroidentifier) [21]–[23].

A. Neuroidentifier (Model Network)

The power system is nonlinear with frequent changes in operating regions due to load changes, disturbances, and setpoint changes. The transactions on the power market and commitments also require the need to change line flows. As the effective series reactance primarily controls the power flow in the line, the settings of the series reactive compensators are required to change according to the line-flow requirement. Also, damping system oscillations require transient changes in the line reactance during the contingency. During these changes of operating conditions, a system identifier can be used to model the system with the measured signals [18], [19].

For HDP neurocontroller designs, neural-network-based one-step-ahead prediction has been found to be sufficient for providing accurate feedback for the action network weight updates [20]–[23]. In this paper, a multilayer perceptron (MLP), shown in Fig. 6, is found to be sufficient for providing an accurate prediction of the system model. The MLP network tracks two remote measurement signals over time. The MLP neuroidentifier consists of ten input linear neurons, a hidden layer with 15 sigmoidal neurons, and an output layer with two linear neurons. The choice of each neural network input linear neurons depends on the number of measurements and number of time-delayed values used for the design. The number of hidden neurons in each network is selected to provide the best tradeoff between computation and accuracy. All of the neural networks in this paper have been trained using a well-known gradient descent-based back-propagation algorithm [26]. For damping control, the system identifier provides a nonlinear model of the system in terms of measured outputs and control inputs. During control signal 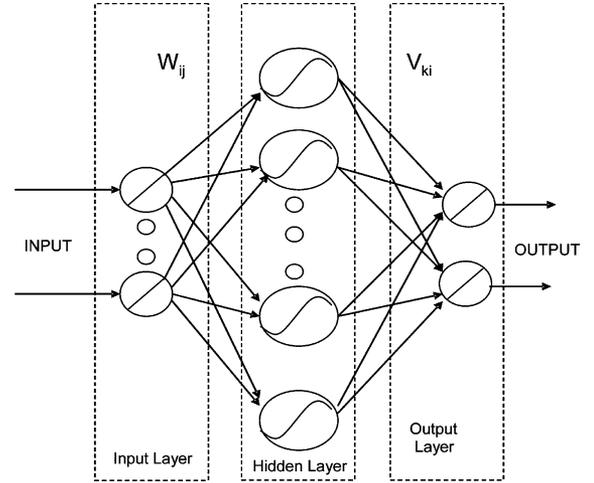generation, the identifier is used to predict the changes in the power or speed oscillations for certain control actions. Moreover, one step-ahead prediction of the identifier is utilized by the critic network to predict the cost-to-go function or sum of future performance indices.

B. HDP Critic Neural Network

The critic network approximates the cost-to-go function J in (2). The critic network is trained forward in time, which is of great importance for real-time optimal control operation (Fig. 7). The ability to foresee future cost and take preventive action ahead of time is important in optimal controller designs. In an optimal control design using dynamic programming, the controller is optimized to provide good performance over a longer period of time. From a dynamic programming point of view, the optimality lies over a time span of actions and results and the performance index is stated as a cost-to-go function. The cost-to-go function is the discounted sum of present and future performance indices. The critic network is trained forward in time to approximate the cost-to-go function. Maximizing or minimizing this function can yield a controller which provides optimal performance over a longer time frame as if the actions taken by the controller can foresee what can be the result of the current action in future times [20].

The ACD techniques use a neural network as an approximating tool to provide an alternative approach to the classical optimal control design. Inherently, both classical- and ACD-based designs are similar as shown in [21]. The target for the critic during the training period is derived from the Bellman's equation (2), as explained in the following derivation (3):

$$
\begin{aligned}
J(t) &= \sum_{k=0}^{\infty} \gamma^k U(t+k) \\
&= U(t) + \sum_{k=1}^{\infty} \gamma^k U(t+k) \\
&= U(t) + \gamma \sum_{k=0}^{\infty} \gamma^k U((t+1)+k) \\
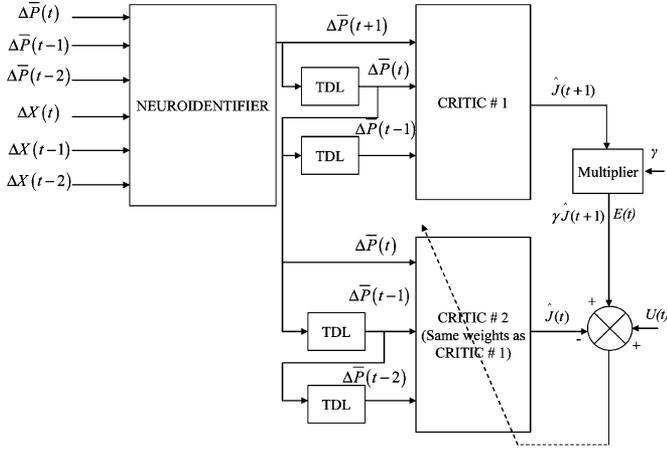&= U(t) + \gamma J(t+1). \quad\quad\quad (3)
\end{aligned}
$$

Fig. 7. HDP critic training.

In the training of the critic network, the objective is to minimize (4)

$$\sum_{t=0}^{\infty} E^2(t) \tag{4}$$

where

$$E(t) = \gamma \hat{J}\left(Y(t+1)\right) + U\left(Y(t)\right) - \hat{J}\left(Y(t)\right). \tag{5}$$

Here, $\hat{J}(t)$ is the estimated cost to go $J(t)$ evaluated by the critic network at time t. The weight updates for the critic network using the standard backpropagation are given by

$$\Delta W_c = \eta_c . E(t) . \frac{\partial \hat{J}\left(Y(t)\right)}{\partial W_c} \tag{6}$$

where η_c and W_c are the learning rate and the weights of the critic neural network, respectively. A detailed explanation for the derivation of the utility function is given in [16]. This utility function U in (2), (3), and (5) plays an important role to form the user-defined optimal cost-to-go function J, and is selected to give the best tradeoff between performance and the control effort. In damping system oscillations, the critic network basically evaluates the area under the oscillating signal beforehand. Thereby, it modulates the control signal to reduce the oscillation amplitude and settling time.

The critic neural network in Figs. 5 and 6 is a three-layer feedforward network with seven input linear neurons, ten sigmoidal neurons in the hidden layer, and one output linear neuron. The critic inputs are the neuroidentifier outputs and their two delayed values. In vector format, it is represented as $\overline{P}(t)$, $\overline{P}(t-1)$, and $\overline{P}(t-2)$ (Fig. 7). The critic or performance evaluator's output is the cost-to-go function $\hat{J}(t)$.

C. Action Network/Optimal Damping Controller

The action network inputs are the power deviation ΔP_3 and ΔP_4 and their two delayed values. An MLP network, similar to that of the identifier and the critic, is used to implement the damping controller. The action MLP consists of 7 input layer linear neurons, 15 sigmoidal neurons in the hidden layer, and one linear neuron in the output layer.

The change in the action network weights (ΔW_A) is calculated by backpropagating a "1" through the trained critic network and then backpropagating the derivative $\partial \hat{J}/\partial \overline{P}$ through the trained neuroidentifier to obtain $\partial J/\partial X$. The error in the action network output is given in (7) where $\hat{Y}_M$ is the output of the neuroidentifier/model

$$e = \frac{\partial \hat{J}}{\partial A} = \left(\frac{\partial \hat{J}}{\partial \hat{Y}_M}\right)\left(\frac{\partial \hat{Y}_M}{\partial A}\right). \tag{7}$$

The weights of the MLP are updated with the backpropagation algorithm [27]. The controller is modified using the feedback from the critic network to improve the cost-to-go function (sum of current and future performance indices). The cost function is chosen to represent system oscillations. Thereby, optimizing the cost function for a damping controller design improves the damping performance of the system.

VI. RESULTS AND DISCUSSIONS

A. HDP-Based Optimal Controller

The HDP-based approach has been proven effective for the optimal control of various devices such as an exciter and turbine. Though the underline technique remains same, the selection of parameters for the training of the HDP critic and action/controller depends on the applications to be used. The value of the discount factor (γ) and the choice of the utility function are critical for optimal performance of the controller.

The neurocontroller is developed in three steps, namely: 1) the neuroidentifier training, 2) critic network training, and the 3) controller network training. The neuroidentifier is trained using forced perturbations (switch S in position 2 in Fig. 3) applied to a specified nominal operating point $(X_{\text{ceff}} = 40.63\ \Omega)$ for the GCSC using pseudorandom binary signals (PRBS) in the range of 0.1 to 0.5 Hz similar to the method described in classical identification methods [28]. In practical systems, a system model can be used to generate disturbance measurements. The ambient measurements due to continuous changes in the system may also be used to train the identifier similar to the classical model identification [29]. The power generated by G3 (P_3) and G4 (P_4) is sampled at 40 Hz to provide the inputs to the neuroidentifier.

The training procedure detailed in [20]–[23] is used for the critic and action training until the weights of the networks do not change significantly. The utility function $U(t)$ given in (8) is chosen to provide the local performance index for optimal controller development

$$U(t) = \left(\Delta P_3(t)^2 + \Delta P_4(t)^2\right). \tag{8}$$

The value of discount factor used for critic training in (5) is 0.6. The choice of discount factor defines optimality over short or long term. If the discount factor is zero, the ACD controller performs similar to the adaptive controller trying to minimize the cost function over one time step. If γ is 1.0, then the controller performance is optimal over an infinite horizon. But equal weighting of present and future performance indices over a longer duration does not improve the transient performance, such as overshoot and settling time. Also, as γ increases, the
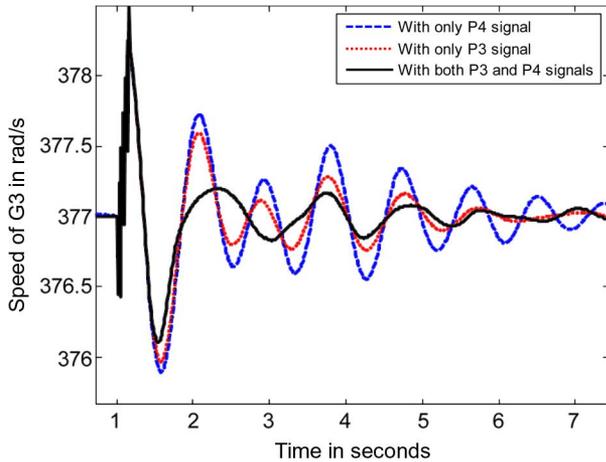
Fig. 8.   Response of G3 speed for a 150 ms 3-Φ fault at bus 3 with different power input signals to the controller.

Fig. 9.   Response of G3 for a 3-Φ short-circuit fault at bus 3 for 150 ms with and without the HDP damping controller.

Fig. 10.   Response of G4 for a 3-Φ short-circuit fault at bus 3 for 150 ms with and without the HDP damping controller.

complexity of the cost function as well as the complexity of the neural network to implement increases. Hence, the choice of γ provides a tradeoff between complexity and optimal performance. In this damping application, $\gamma = 0.6$ shows very good performance for overshoot and settling time with reasonable size and complexity of the neural networks. Theoretically, with a γ of 0.6, the effect of controller action reduces to 1% within ten time steps.

The initial weights of the controller network are those that can provide stabilizing control at one operating point. These weights are obtained using the indirect adaptive control method [16]. Obtaining the initial weights of the action network are known as pretraining of the neurocontroller. After pretraining of the neurocontroller, the controller is trained using the feedback from the critic network. The critic and controller training are interleaved. Once the controller network weights have converged for a number of operating conditions, the weights are frozen and the neurocontroller is left online with the system. Though the computational effort is high during an initial phase of offline design, after the finalization of the controller, the parameters of the controller are fixed (similar to linear controllers). Hence, the implementation of the controller in real time can be accomplished using less expensive microprocessors.

B. Discussion of Simulation Results

To observe the performance of the proposed optimal control method, different disturbances are applied to the system. The objective of the HDP controller is to damp out the oscillations arising from different disturbances. Linear analysis of the 12-bus system suggests that the effect of the line flow in 7–8 has little effect on the modes of generators G2 and G4. Hence, the damping provided by the optimal controller is mostly visible in generator G3. Fig. 8 shows the speed response of G3 for a 150 ms 3-Φ short circuit at bus 3 with P_3, P_4, and P_3, and P_4 signals as inputs to the damping controller. This figure shows that the remote measurement signal from G4 (P_4) has a significant effect on the performance of the controller. Thus, the use of both remote signals P_3 and P_4 can be justified for the optimal damping controller design.

Figs. 9 and 10 present the speed responses of G3 and G4 for the aforementioned fault, with and without the HDP optimal
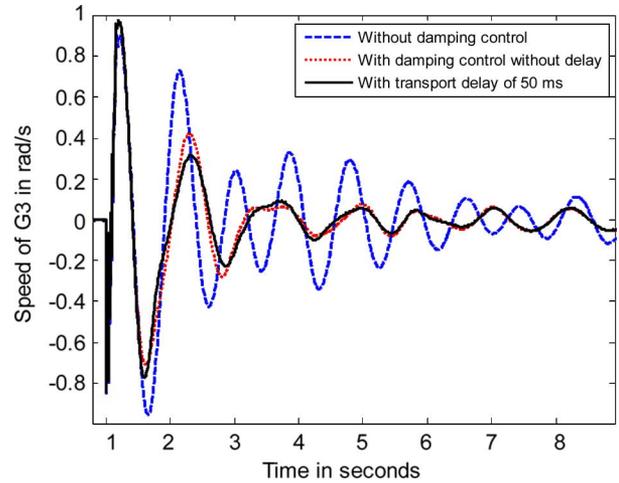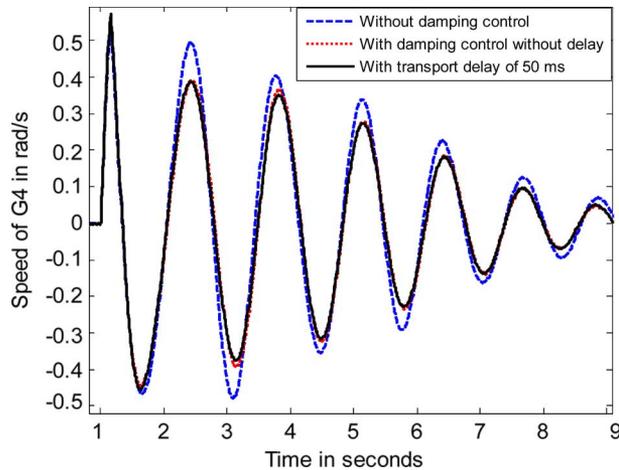
damping controller. The damping in the response of generator G3 is significantly enhanced with the proposed controller. A transport delay of 50 ms in the measured signal is also simulated and it can be seen from Figs. 9 and 10 that there is no effect in the performance as assumed during the design. Fig. 11 shows the active power flow in line 7–8 due to the same short-circuit fault. The enhanced damping in the power oscillation is also visible with the HDP controller. Fig. 12 shows the respective control signal generated by the damping controller during the short-circuit disturbance and it is within the limits specified by -40 to $60 \ \Omega$.

In a second test, one line between bus 3 and 4 is removed to represent a different operating condition. Fig. 13 shows the effect on generator G3 due to this line outage. The time-domain simulation exhibits a similar enhancement of damping in generator G3 as experienced under the short-circuit fault. A 50-ms transport delay in the measured signal has shown no effect on the performance. Fig. 14 presents the effect on the speed of generator G3 due to a different contingency where a line outage is simulated between buses 4 and 6.

All these results show improvement in damping as a result of a remote signal-based optimal controller even with a small transport delay (typically <50 ms). Hence, the proposed offline
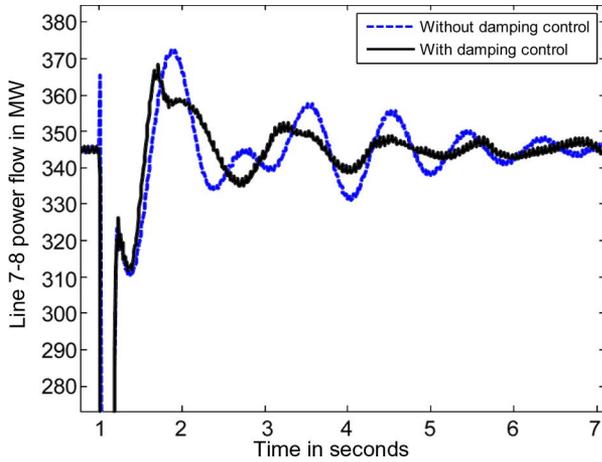
Fig. 11. Power oscillation in line 7–8 for a 3-Φ short-circuit fault at bus 3 for 150 ms with and without the HDP damping controller.

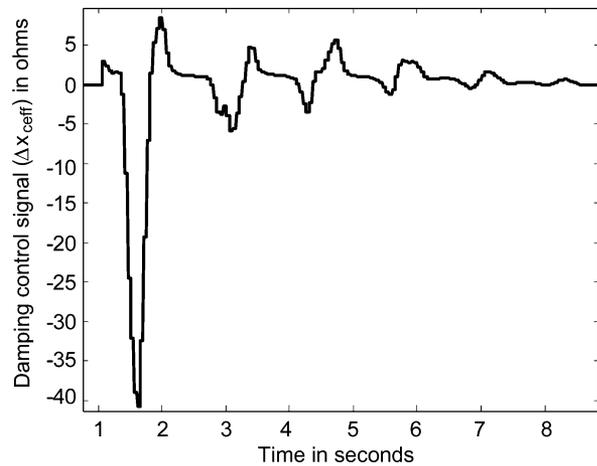Fig. 12. Control signal (ΔX_{ceff}) for 3-Φ short-circuit fault at bus 3 for 150 ms with an HDP damping controller.
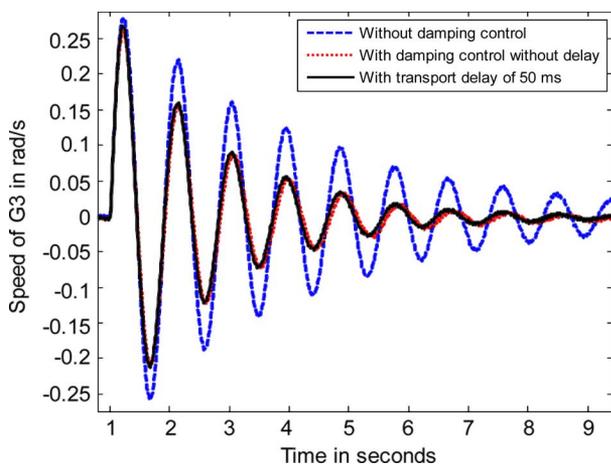

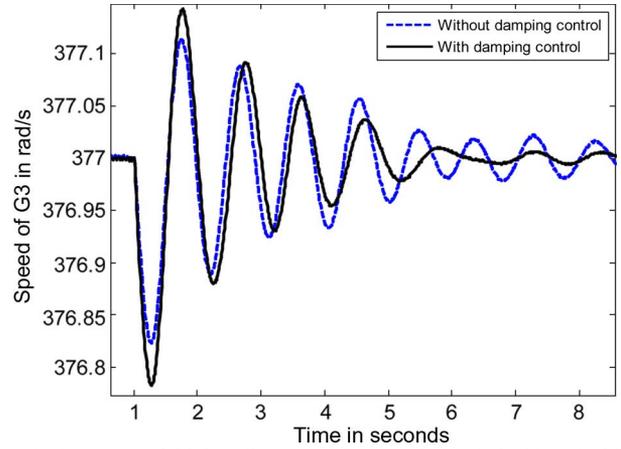Fig. 13. Response of G3 for a line outage between buses 3–4.

Fig. 14. Response of G3 for a line outage between buses 4–6 with and without the HDP damping controller.

TABLE II
FREQUENCIES AND DAMPING OF DOMINANT MODES
FROM G3 SPEED DATA FOR 150-ms SHORT CIRCUIT

WITHOUT CONTROL		WITH HDP CONTROL	
FREQ (HZ)	DAMPING	FREQ (HZ)	DAMPING
0.92	27%	0.84	65%
1.12	5%	1.16	12%

TABLE III
FREQUENCIES AND DAMPING OF DOMINANT MODES FROM G3
SPEED DATA FOR A LINE OUTAGE BETWEEN BUSES 3 AND 4

WITHOUT CONTROL		WITH HDP CONTROL	
FREQ (HZ)	DAMPING	FREQ (HZ)	DAMPING
0.86	7%	0.83	9%
1.10	4%	1.09	8%

C. Evaluation of Damping Performance

Prony analysis [30] is an extension of the Fourier analysis and it helps to find the modal contents by estimating frequency, damping, and phase of a signal. Responses under different fault conditions are investigated with the Prony method. Comparisons in Tables II and III show the improvement in damping with the HDP controller for short-circuit and line-outage faults. Table II shows that for the nominal operating condition with a large disturbance (150-ms short circuit), the HDP controller provides a 7% improvement in damping for the least damped mode of 1.12 Hz. Table III shows a 4% improvement for the least damped mode of 1.1 Hz. The effect on G4 is minimal as the line flow in line 7–8 (GCSC location) does not participate significantly in G4 oscillations.

VII. CONCLUSION

This paper has presented a computational technique for an offline design of an optimal damping controller using the HDP approach. This computational approach is mainly measurement

measurement-based technique is a promising optimal controller design. A similar technique can also be applied to larger power systems without major modifications. This paper has only verified the design on a FACTS benchmark system [24]. In the next section, quantitative evaluation of dampings is presented using the Prony method.

based and no linear model of the system needs to be developed unlike classical optimal designs. The HDP-based optimal controller design can be accomplished by using the available measurement data from real (practical) systems. In this paper, an optimal damping controller, using remote measurements, for a GCSC is used to provide damping of system modes. Neural networks have been used as agents to develop an optimal control law using the proposed method. The design yields a fixed weight nonlinear controller which is easier to implement in practical systems than adaptive controllers.

The study of the proposed control strategy shows the effectiveness of the HDP-based optimal controller for oscillation damping. The GCSC, as a relatively inexpensive and simpler power-flow control device, has a lot of potential to be introduced in locations where fixed capacitors or other series FACTS devices are currently used. The proposed nonlinear controller provides an alternate design to classical approaches to provide stability to the compensated system.

Real-time implementation and testing using a real-time digital simulator (RTDS) will be continued in the future. The future work will also involve inclusion of frequency-domain characteristics in the utility or objective function.

REFERENCES

[1] C. Gama, "Brazilian North-South interconnection control-application and operating experience with a TCSC," in *Proc. IEEE Power Eng. Soc. Summer Meeting*, Jul. 1999, vol. 2, pp. 1103–1108.

[2] J. F. Hauer, W. A. Mittelstadt, R. J. Piwko, B. L. Damsky, and J. D. Eden, "Modulation and SSR tests performed on the BPA 500 kV thyristor controlled series capacitor unit at Slatt substation," *IEEE Trans. Power Syst.*, vol. 11, no. 2, pp. 801–806, May 1996.

[3] L. F. W. de Souza, E. H. Watanabe, and M. Aredes, "GTO controlled series capacitor," in *Proc. IEEE Power Eng. Soc. Winter Meeting*, Jan. 2000, vol. 4, pp. 2520–2525.

[4] L. F. W. de Souza, E. H. Watanabe, J. E. R. Alves, and L. A. S. Pilotto, "Thyristor and gate controlled series capacitors: Comparison of components rating," in *Proc IEEE Power Eng. Soc. General Meeting*, Jul. 2003, vol. 4, pp. 2542–2547.

[5] L. F. W. de Souza, E. H. Watanabe, and M. Aredes, "GTO controlled series capacitors: Multi-module and multi-pulse arrangements," *IEEE Trans. Power Del.*, vol. 15, no. 2, pp. 725–731, Apr. 2000.

[6] F. A. L. Jowder, "Influence of mode of operation of the SSSC on the small disturbance and transient stability of a radial power system," *IEEE Trans. Power Syst.*, vol. 20, no. 2, pp. 935–942, May 2005.

[7] X.-P. Zhang, "Advanced modeling of the multicontrol functional static synchronous series compensator (SSSC) in newton power flow," *IEEE Trans. Power Syst.*, vol. 18, no. 4, pp. 1410–1416, Nov. 2003.

[8] R. E. Wilson and C. W. Taylor, "Using dynamic simulations to design the wide-area stability and voltage control system (WACS)," in *Proc. IEEE Power Systems Conf. Expo.*, Oct. 2004, vol. 1, pp. 100–107.

[9] M. E. Aboul-Ela, A. A. Sallam, J. D. McCalley, and A. A. Fouad, "Damping controller design for power system oscillations using global signals," *IEEE Trans. Power Syst.*, vol. 11, no. 2, pp. 767–773, May 1996.

[10] M. Zima, M. Larsson, P. Korba, C. Rehtanz, and G. Andersson, "Design aspects for wide-area monitoring and control systems," *Proc. IEEE*, vol. 93, no. 5, pp. 980–996, May 2005.

[11] D. Karlsson, M. Hemmingsson, and S. Lindahl, "Wide area system monitoring and control-terminology, phenomena, and solution implementation strategies," *IEEE Power Energy Mag.*, vol. 2, no. 5, pp. 68–76, Sep./Oct. 2004.

[12] I. C. Decker, D. Dotta, M. N. Agostini, S. L. Zimath, and A. S. de Silva, "Performance of a synchronized phasor measurements system in the Brazilian power system," presented at the IEEE Power Eng. Soc. General Meeting, Jun. 2006.

[13] K. E. Martin, "Phasor measurement systems in the WECC," presented at the IEEE Power Eng. Soc. General Meeting, Jun. 2006.

[14] B. Choudhuri, R. Majumder, and B. C. Pal, "Application of multiple-model adaptive control strategy for robust damping of interarea oscillations in power system," *IEEE Trans. Contr. Syst. Technol.*, vol. 12, no. 5, pp. 727–736, Sep. 2004.

[15] R. Majumder, B. C. Pal, C. Dufour, and P. Korba, "Design and real-time implementation of robust FACTS controller for damping inter-area oscillation," *IEEE Trans. Power Syst.*, vol. 21, no. 2, pp. 809–816, May 2006.

[16] G. K. Venayagamoorthy and R. P. Kalyani, "Two separate continually online trained neurocontrollers for a unified power flow controller," *IEEE Trans. Ind. Appl.*, vol. 41, no. 4, pp. 906–916, Jul. 2005.

[17] P. K. Dash, S. Mishra, and G. Panda, "A radial basis function neural network controller for UPFC," *IEEE Trans. Power Syst.*, vol. 15, no. 4, pp. 1293–1299, Oct. 2000.

[18] J. W. Park, R. G. Harley, and G. K. Venayagamoorthy, "New external neuro-controller for series capacitive reactance compensator in a power network," *IEEE Trans. Power Syst.*, vol. 19, no. 3, pp. 1462–1472, Aug. 2004.

[19] G. K. Venayagamoorthy and R. G. Harley, "Two separate continually online-trained neurocontrollers for excitation and turbine control of a turbogenerator," *IEEE Trans. Ind. Appl.*, vol. 38, no. 3, pp. 887–893, May/Jun. 2002.

[20] J. Si, A. Barto, W. Powell, and D. C. Wunsch, *Handbook of Learning and Approximate Dynamic Programming*. New York: Wiley, Jul. 2004, 0-471-66054-X.

[21] P. Jung-Wook, R. G. Harley, and G. K. Venayagamoorthy, "Adaptive-critic-based optimal neurocontrol for synchronous generators in a power system using MLP/RBF neural networks," *IEEE Trans. Ind. Appl.*, vol. 39, no. 5, pp. 1529–1540, Sep./Oct. 2003.

[22] G. K. Venayagamoorthy, R. G. Harley, and D. C. Wunsch, "Comparison of heuristic dynamic programming and dual heuristic programming adaptive critics for neurocontrol of a turbogenerator," *IEEE Trans. Neural Netw.*, vol. 13, no. 3, pp. 764–773, May 2002.

[23] G. K. Venayagamoorthy, R. G. Harley, and D. C. Wunsch, "Dual heuristic programming excitation neurocontrol for generators in a multimachine power system," *IEEE Trans. Ind. Appl.*, vol. 39, no. 2, pp. 382–394, Mar./Apr. 2003.

[24] S. Jiang, U. D. Annakkage, and A. M. Gole, "A platform for validation of FACTS models," *IEEE Trans. Power Del.*, vol. 21, no. 1, pp. 484–491, Jan. 2006.

[25] S. Mohagheghi, G. K. Venayagamoorthy, and R. G. Harley, "Optimal wide area controller and state predictor for a power system," *IEEE Trans. Power Syst.*, vol. 22, no. 2, pp. 693–705, May 2007.

[26] Manitoba HVDC Research Centre Inc., PSCAD/EMTDC User's Guide ver. 3.0, 244 Cree Crescent. Winnipeg, MB, Canada.

[27] P. Werbos, *Roots of Backpropagation*. New York: Wiley, 1994.

[28] N. Zhou, J. W. Pierre, and J. F. Hauer, "Initial results in power system identification from injected probing signals using a subspace method," *IEEE Trans. Power Syst.*, vol. 21, no. 3, pp. 1296–1302, Aug. 2006.

[29] J. W. Pierre, D. J. Trudnowski, and M. K. Donnelly, "Initial results in electromechanical mode identification from ambient data," *IEEE Trans. Power Syst.*, vol. 12, no. 3, pp. 1245–1251, Aug. 1997.

[30] J. F. Hauer, "Application of Prony analysis to the determination of modal content and equivalent models for measured power system response," *IEEE Trans. Power Syst.*, vol. 6, no. 3, pp. 1062–1068, Aug. 1991.

Swakshar Ray (S'02) received the B.E. degree (Hons.) in electrical engineering from Jadavpur University, Calcutta, India, in 2000, and the M.S. degree in electrical engineering from Oklahoma State University, Stillwater, in 2003, and is currently pursuing the Ph.D. degree at the University of Missouri–Rolla.

He was a Commissioning Engineer in the Control and Automation Division with Larsen and Toubro India Ltd., Mumbai, India, from 2000 to 2001. He is a member of the Real-Time Power and Intelligent Systems (RTPIS) Laboratory, University of Missouri-Rolla. His research interests are in control systems, power systems, computational intelligence, and signal processing.

Mr. Ray is the recipient of the Hughes Scholarship from the Department of Electrical and Computer Engineering, Oklahoma State University, in 2003 and the IEEE Computational Intelligence Society (CIS) W. J. Karplus summer research grant in 2005. He has been awarded 2nd prize in the Power Engineering Society Student Poster Contest at the 2007 Power Engineering Society General Meeting. He is also a member of the Task Force on Intelligent Control Systems of IEEE power engineering society and is a student member of the IEEE Industrial Automation Society.

Ganesh Kumar Venayagamoorthy (S'91–M'97–SM'02) received the B.Eng. degree (Hons/) in electrical and electronics engineering from Abubakar Tafawa Balewa University, Bauchi, Nigeria, in 1994, and the M.Sc.Eng. and Ph.D. degrees in electrical engineering from the University of Natal, Durban, South Africa, in 1999 and 2002, respectively.

He was a Senior Lecturer with Durban Institute of Technology, Durban, South Africa, prior to joining the University of Missouri, Rolla (UMR), in 2002. Currently, he is an Associate Professor of Electrical and Computer Engineering and the Director of the Real-Time Power and Intelligent Systems Laboratory at UMR. He was a Visiting Researcher at the ABB, Corporate Research Center, Vasteras, Sweden, in 2007. His research interests are in the development and applications of computational intelligence for real-world applications, including power systems stability and control, FACTS devices, power electronics, alternative sources of energy, sensor networks, collective robotic search, signal processing and evolvable hardware. He has published two edited books, three book chapters, 55 refereed journals papers, and 200 refereed international conference proceeding papers. Dr. Venayagamoorthy was an Associate Editor of the IEEE TRANSACTIONS ON NEURAL NETWORKS and the IEEE TRANSACTIONS ON INSTRUMENTATION AND MEASUREMENT. He is a Senior Member of the South African Institute of Electrical Engineers (SAIEE) and a member of the International Neural Network Society (INNS), The Institution of Engineering and Technology, U.K., and the American Society for Engineering Education. Currently, he is the IEEE St. Louis Computational Intelligence Society (CIS) and IAS Chapter Chairs, the Chair of the Working Group on Intelligent Control Systems, the Secretary of the Intelligent Systems subcommittee and the Vice-Chair of the Student Meeting Activities subcommittee of the IEEE Power Engineering Society, and the Chair of the IEEE CIS Task Force on Power System Applications. He has organized and chaired several panels, invited and regular sessions, and tutorials at international conferences and workshops.

Dr. Venayagamoorthy was a recipient of the 2007 ONR Young Investigator Program Award, the 2004 Natiojnal Science Foundation CAREER Award, the 2006 IEEE Power Engineering Society Walter Fee Outstanding Young Engineer Award, the 2006 IEEE St. Louis Section Outstanding Section Member Award, the 2005 IEEE Industry Applications Society (IAS) Outstanding Young Member Award, the 2005 SAIEE Young Achievers Award, the 2004 IEEE St. Louis Section Outstanding Young Engineer Award, the 2003 INNS Young Investigator Award, the 2001 IEEE CIS Walter Karplus Summer Research Award, five prize papers from the IEEE IAS and IEEE CIS, a 2006 UMR School of Engineering Teaching Excellence Award, and a 2005 UMR Faculty Excellence Award. He is listed in the 2007 and 2008 editions of *Who's Who in America*, 2008 edition of *Who's Who in the World* and 2008 edition of *Who's Who in Science and Engineering*.

Edson H. Watanabe (M'76–SM'02) was born in Rio de Janeiro, Brazil, on November 7, 1952. He received the Electronic Engineer and M.Eng. degrees from the Federal University of Rio de Janeiro, Rio de Janeiro, Brazil, in 1975 and 1976, respectively, and the D.Eng. degree from the Tokyo Institute of Technology, Tokyo, Japan, in 1981.

He became an Associate Professor at COPPE/Federal University of Rio de Janeiro, in 1981, and a Professor at COPPE/Federal University of Rio de Janeiro in 1993, where he teaches power electronics. His main fields of interests are converters analysis, modeling and design, active filters, and FACTS technologies.

Dr. Watanabe is a member of the Institute of Electrical Engineers–Japan, The Brazilian Society for Automatic Control, The Brazilian Power Electronics Society, CIGRE and Power Engineering, Industry Applications and Power Electronics Societies of IEEE. In 2005, he was admitted to the National Order of Scientific Merit, Brazil.